Results from Navigator GPS Flight Testing for the Magnetospheric MultiScale Mission

Tyler D. Lulich, *Emergent Space Technologies*
Dr. William A. Bamford, *Emergent Space Technologies*
Dr. Luke M. B. Winternitz, *NASA-GSFC*
Samuel R. Price, *NASA-GSFC*

BIOGRAPHY

Tyler Lulich is an Aerospace Engineer at Emergent Space Technologies, and has been involved with Navigator development and testing for the past two years. He holds a B.S. in Mech. Eng. from Milwaukee School of Engineering (2006) and an M.S. in Eng. from the School of Aeronautics and Astronautics at Purdue University (2010).

Dr. William Bamford received his Ph.D. from the University of Texas at Austin in 2004, at which time he was hired by Emergent. He has worked on development and testing of the Navigator receiver for the past six years as well as performing GPS-based navigation studies for Orion, F6 and GOES-R.

Dr. Luke Winternitz is an engineer in NASA-GSFC's GN&C hardware components branch space-GPS receiver research and development group. He is one of the technical leads of the Navigator GPS program. He holds a B.S in Mathematics and Elec. Eng. (2001) and an M.S (2007) and Ph.D. (2010) in Elec. Eng. all from the University of Maryland, College Park.

Sam Price received a B.S in Com. Sci. from Western Illinois University (2005) and a B.S in Elec. Eng. from Bradley University, IL (2009) with an emphasis on software defined GPS receivers. He joined NASA-GSFC's GN&C hardware components branch in 2009, and has been developing the flight software for Navigator GPS.

ABSTRACT

The recent delivery of the first Goddard Space Flight Center (GSFC) Navigator Global Positioning System (GPS) receivers to the Magnetospheric MultiScale (MMS) mission spacecraft is a high water mark crowning a decade of research and development in high-altitude space-based GPS. Preceding MMS delivery, the engineering team had developed receivers to support multiple missions and mission studies, such as Low Earth Orbit (LEO) navigation for the Global Precipitation Mission (GPM), above the constellation navigation for the Geostationary Operational Environmental Satellite (GOES) proof-of-concept studies, cis-Lunar navigation with rapid re-acquisition during re-entry for the Orion Project and an orbital demonstration on the Space Shuttle during the Hubble Servicing Mission (HSM-4).

INTRODUCTION

Recently, the first Navigator Global Positioning System (GPS) receivers were delivered for integration to the Magnetospheric MultiScale (MMS) mission spacecraft at Goddard Space Flight Center (GSFC). This milestone is the culmination of many years of GPS receiver research and development activities at GSFC, towards the goal of expanding the utility of GPS to challenging new space applications well beyond low Earth orbit (LEO).

The MMS mission consists of four identical, tuna-can shaped spacecraft designed to investigate magnetic reconnection of the Earth's magnetosphere in very highly elliptical orbits known as Phase 1 & 2 with perigee at 1.2 R_E and apogee at 12 and 25R_E, respectively. Navigation performance requirements stem from the need to control the relative positions of the satellites in a desired formation, while protecting against conjunctions between the satellites. The Navigator receiver includes a capability to acquire and track very weak GPS signals, and incorporates an ultra-stable reference oscillator (USO) and internal extended Kalman filter to meet navigation and timing performance requirements in the presence of sparse GPS signal availability. The receiver is designed to survive the harsh radiation environment present in high Earth orbits. Finally, the MMS implementation required a customized radio-frequency (RF) design and features to allow tracking of the GPS signals via four independent antennas spaced radially around the perimeter of the spinning spacecraft.

The design of the Navigator receiver hardware and software has been documented in several references [**1**] [**2**] [**3**] and will not be repeated here. Instead, this paper will focus on the test setup of GSFC's Formation Flying Testbed (FFTB), a state-of-the-art facility for the testing and analysis of hardware-in-the-loop navigation, used for MMS testing, and a summary of the MMS testing results.

NAVIGATOR GPS PROGRAM

NASA Goddard's GN&C hardware components branch initiated a spaceflight GPS receiver development program in the mid 1990's. GSFC led one of the early flight high Earth orbit GPS experiments, operating a GPS receiver on the AMSAT-OSCAR-40 satellite which recorded measurements of the GPS side lobe signals [**4**]. GSFC then leveraged a popular commercial GPS chipset to create the PiVoT GPS receiver, which was used as a development platform, and on Balloon experiments. As the program progressed, high-altitude space-based GPS navigation, above the GPS constellation itself, emerged as a focus area [**5**] [**6**]. In the early 2000's the Navigator GPS receiver program was initiated to create a GPS receiver specifically designed for Geostationary and other high-altitude applications [**1**] [**2**] [**3**]. On the way to the development of the MMS-Navigator, shown mechanically integrated to the first spacecraft bus in Figure 1, related receivers were built in support of multiple missions and mission studies, including the LEO Global Precipitation Measurement (GPM) mission, above the constellation navigation for the Geostationary Operational Environmental Satellite (GOES) proof of concept studies, cis-Lunar navigation with rapid re-acquisition during re-entry for the Orion Project, and an orbital demonstration on the Space Shuttle during the Hubble Servicing Mission (HSM-4) [**7**].

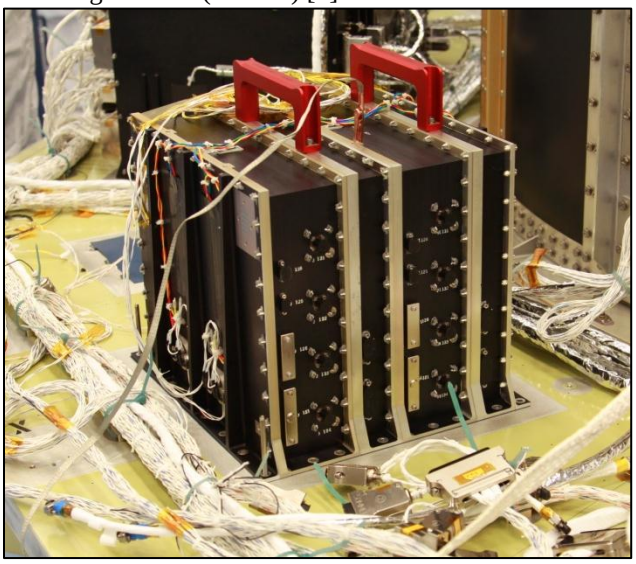

Figure 1: Fully redundant Navigator box mechanically integrated onto MMS spacecraft #1.

THE MAGNETOSPHERIC MULTISCALE MISSION

The MMS mission consists of four nearly identical, tuna-can shaped spacecraft designed to investigate magnetic reconnection of the Earth's magnetosphere in two regions of interest (RoI), from 9 to $12R_E$ and 18 to $25R_E$, respectively. The spacecraft will spin at a nominal rate of three revolutions per minute (RPM) and vary in formation configuration from a tetrahedron in the RoIs, near apogee, to a linear "string-of-pearls" configuration at perigee. Two highly elliptical orbits known as Phase 1 ($1.2\text{x}12R_E$) and Phase 2 ($1.2\text{x}25R_E$) have been designed to enable scientific observations in the two RoIs. [**8**]

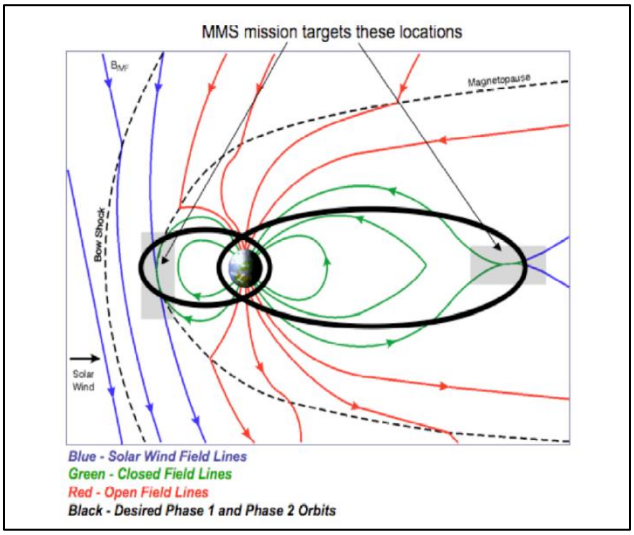

Figure 2: Regions of interest in the MMS orbit [8**].**

Fully redundant Navigator GPS receivers on each spacecraft will track L1C/A code GPS signals in order to provide absolute position, velocity, and time (PVT) estimates to the spacecraft and ground system. PVT estimates are produced continuously, in real-time, by the Goddard Enhanced Onboard Navigation System (GEONS), an integrated extended Kalman filter, which allows measurement updates even when fewer than four GPS signals are tracked, and high fidelity onboard state propagation during measurement outages. Traditional point-positioning techniques are also used, when sufficient numbers of signals are visible, to initialize and monitor the filter performance. The filtered solution is used by the navigation ground system and science team, and the time estimate is distributed in real time onboard via a one pulse-per-second (PPS) signal and an associated time-of-tone telemetry packet.

The MMS-Navigator software and hardware have been specially designed to meet and exceed MMS mission requirements for tracking both weak and strong L1C/A GPS signals from a spinning platform. A key to Navigator's excellent performance is its ability to autonomously and rapidly acquire weak GPS signals with received carrier-to-noise density (C/N_0) levels down to 25dB-Hz, including those emerging from the transmitter antenna side-lobes. This capability is achieved by the use of its specialized acquisition engine, described in [**2**]. Figure 3 and Figure 4 depict the range of visibility of the GPS main-lobes and side-lobes antenna patterns to a receiver with assumed 35 and 25dB-Hz sensitivity, respectively.

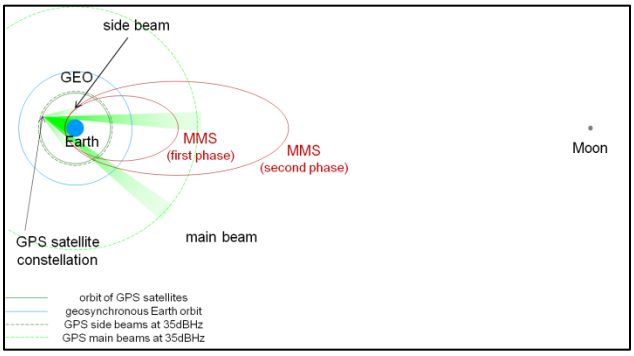

Figure 3: 35dB-Hz sensitivity.

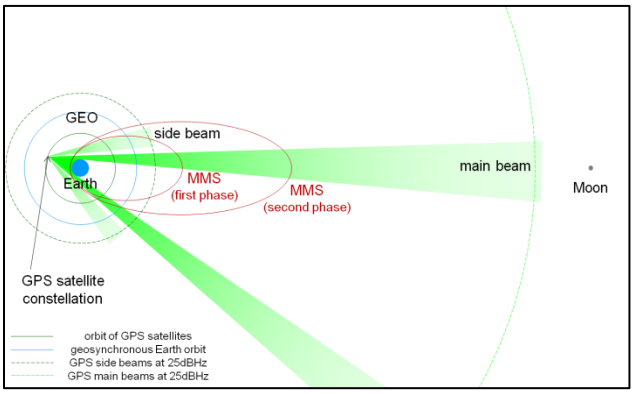

Figure 4: 25 dB-Hz sensitivity.

The remainder of the paper is organized as follows. We first describe the test facility, Goddard's Formation Flying Testbed (FFTB), including its capabilities and configuration for MMS testing. Next we describe the mission requirements and test plan developed to verify these requirements. Finally, we present results from the executed test plan, present some lessons-learned in developing and testing the MMS-Navigator, and draw conclusions.

FORMATION FLYING TESTBED

Goddard's FFTB is a state-of-the-art test facility developed for hardware-in-the-loop validation of formation flying navigation sensors and systems. It is equipped with a full range of RF test equipment including an array of GPS constellation and RF crosslink channel simulators. The FFTB has supported the testing of navigation sensors for many NASA and outside missions including ST9, HST-SM4, Constellation/Orion, GPM, MMS, GOES-R, Firefly, AFRL ANGELS, to name a few [**9**][**8**][**10**][**11**]. The FFTB has also been the primary development lab for the Navigator GPS receiver program.

For testing of the MMS GPS receivers, the FFTB has primarily relied on its array of Spirent STR4760 GPS constellation simulators to generate the L1C/A GPS signals which Navigator will expect to acquire and track on-orbit. To allow continuous tracking of GPS signals from the spinning spacecraft, each MMS vehicle is equipped with four independent GPS antennas, spaced at 90º offsets around the perimeter of the vehicle, the feeds of which are processed by four independent RF chains and analog-to-digital converters in the GPS receivers. Obstructions on the top and bottom of the spacecraft, coupled with mission attitude control requirements precluded a simpler two-antenna solution. Therefore, the receiver was designed to track the GPS signals as they transition between the four perimeter antennas, approximately every 5 seconds for a 3 RPM spin rate. The high sensitivity requirement precluded analog combining of the four perimeter antennas.

To simulate this configuration, a pair of dual-output Spirent STR4760 GPS constellation simulators, synchronized to a lab Cesium frequency standard, are setup in a master-slave mode to simulate signals for each of the four GPS antennas. Accurate MMS spacecraft orbits and attitude time-histories are provided to these "Spirent racks" at a 10Hz update rate to provide a high fidelity RF simulated environment to test the GPS receivers.

In order to fully test the performance of the receiver, particularly that of the embedded Kalman filter GEONS, a minimum of three complete orbits were simulated. The MMS Phase 2 orbit has a period of approximately 2.8 days, and since the testing proceeds in real-time, the Phase 2 simulations must run for a minimum of eight days to produce a sufficient dataset. Achieving successful simulations of this length under schedule pressure was a major challenge for the test team. The MMS test program had to overcome power outages, severe weather, simulator failures, HVAC malfunction, and humidifier-generated electromagnetic pulses, to name a few.

Customized parameters used to define the GPS constellation simulation include transmitter antenna gain pattern, receiver antenna gain and phase pattern, ionosphere model, fine signal strength settings, and a file defining the spacecraft orbit and attitude time-history. The geometry of the orbits implies that a large number of visible signals will be seen from the side lobes of the transmitter pattern and indeed, use of these signals is a key to successful GPS navigation for MMS. The levels of these side-lobe signals are known to vary significantly between GPS transmitters and are known to have significant variation in azimuth in each individual antenna pattern. The Block IIR-M transmitter patterns have been used in MMS-Navigator testing, as they provide perhaps the best representation of the signals present across the GPS constellation, and provide a conservative representation of side-lobe signal levels. The receiver antenna gain and phase patterns were generated by the MMS GPS antenna design team using high fidelity electromagnetic models of the MMS antennas on the

MMS spacecraft. Finally, a significant effort was made to achieve an accurate, yet reasonably conservative, calibration of the Spirent signal levels in order to ensure that the C/N_0 levels seen by the receiver-under-test match predicted levels on-orbit, for different test configurations. This is perhaps the most critical setting for the simulation because slight inaccuracies in its setting, producing received power levels either slightly higher or slightly lower than realistic conditions, can significantly affect navigation performance achieved. The next section is dedicated to discussing how this signal level was calibrated.

SIGNAL LEVEL CALIBRATION

This calibration boils down to careful selection of the simulator's "global gain" parameter which is applied to all transmitter-to-receiver links. This parameter can be used to compensate for differences in the lab and on-orbit system noise temperature and to account for assumptions in the simulator link model that may not accurately model the on-orbit situation. Table 1 displays an example (actual numbers not important for this discussion) breakdown of the terms contributing to the global gain adjustment.

The first term in the table is the receiver noise adjustment. To compute this term, we predicted the on-orbit system noise temperature using flight hardware noise and passive loss specifications, and an estimated antenna noise of 90K (based on a certain average of 30K space and 290K Earth temperatures). The lab system noise temperature was estimated based on a 290K simulator antenna temperature, noise specifications for the engineering-unit LNA, and careful accounting of passive losses.

The next five terms in the Table have to do with the simulator link model. There are adjustments for differing definitions of the "Reference Range" and an associated off-boresite transmit angle and gain between IS-GPS-200F [**12**] and the Spirent User Manual [**13**]. Another adjustment removes an atmospheric attenuation term that does not apply in space. The receiver antenna peak gain is then accounted for (as our receive antenna models are generally given as attenuation patterns). Next, some gain is removed for expected, but unmodeled, polarization losses in the transmit antenna side-lobes. (Including this term in the "global gain" makes signals received from the transmit antenna main lobe somewhat lower than expected, but we prefer this to providing too much signal in the side-lobes.) Another term accounts for average excess gain of the (Block IIR) GPS transmitter above specified levels.

Finally we account for attenuators affixed to the Spirent output ports. These are in place to keep the global gain near its upper limit. This term could have been accounted for in the receiver noise adjustment term, but we prefer to account for it separately.

To verify this global gain calibration procedure, the same general procedure was applied to set the global gain for a rooftop-mounted MMS engineering test unit (ETU) antenna and LNA/passive loss configuration. A Spirent simulation was then set up to model the rooftop scenario for the current date. Reported C/N_0 levels from the simulation were compared to those estimated from the live-sky signals received by the antenna and showed to be in very good agreement (neglecting multipath variations and low-elevation signals).

The analysis conducted for the global gain calibration was also importantly used to calibrate the link model used to simulate GPS measurements in the MMS flight dynamics team's offline orbit-determination Monte-Carlo simulations [**14**].

Table 1: MMS global gain adjustments

Source
1. Rx noise adjust
2. Reference Range
3. Tx Antenna Gain
4. Atmosphere
5. Rx Antenna Gain
6. Polarization Loss
7. Excess Gain
8. Fixed Attenuators

PERFORMANCE REQUIREMENTS AND TEST PLAN

The key performance requirements levied on the MMS-Navigator are summarized in the list below. These requirements are either directly related to the MMS primary navigation requirements [**15**], or are in place to ensure consistency with the associated GEONS offline Monte Carlo simulations [**14**].

- Align PPS to TAI time within 325 μs
- Maintain semimajor axis (SMA) error less than 100m (above 3 R_E)
- Acquire signals at or below -175 dBW
- Track signals at or below -172 dBW
- Acquire 95% of signals with received power greater than -156 dBW, and 75% of signals with received power less than -156 dBW
- Acquire and track signals with a dynamic range of at least 15 dB
- Maintain measurement noise less than 30 m (3σ)

In order to verify these primary requirements, a series of tests were developed and assembled into a coherent test plan. Laboratory resources were organized in attempt to meet the scheduled delivery of hardware to the spacecraft level. In general, each receiver must individually pass the

full system and benchmark tests; however, corner-case tests need only be demonstrated once because they either validate software or verify performance beyond normal requirements.

Simulation data processing tools were developed and revision controlled to ensure repeatability of the analysis of each dataset. The processing tools go well beyond simply verifying requirements. For each simulation, critical telemetry from the receiver is carefully checked to ensure it meets expectations and compares well with agreed upon performance standards, which are generally derived from prior, pre-validated simulations

KEY TEST DESCRIPTION AND RESULTS

In this section we describe and present example results from a subset of the tests run on the MMS-Navigator GPS Flight Box 1-Side A. This subset includes two full system tests (Phase 1, Phase 2B), two benchmark tests (Measurement Noise, Acquisition Probability), and one corner-case test (High Spin Rate).

Table 2 lists dynamic modeling parameters used in both generation of truth trajectory, and modeled in the GEONS filter during full system testing. Differences between truth and GEONS model parameters are intended to be representative of dynamic modeling errors that will be present during the actual mission.

Table 2: Parameters for the Full System Tests [14].

Parameter	Truth	Filter
Non-Spherical Earth Gravity Model	21x21 EGM-96	13x13 JGM2
Point Mass Gravity	Sun, Moon using DE 405 ephemeris	Sun, Moon using analytical fit to DE 404 ephemeris, with 30 sec min lunar update interval
Atmospheric Drag	Jacchia Roberts, Schatten +2 sigma prediction solar flux, C_D of 2.2, Drag area of 7.1 m^2	Analytical fit to Harris Priester model, C_D of 2.2, Drag area of 7.1 m^2
Solar Radiation Pressure	Spherical model, C_R of 1.8, SRP area of 2.026712 m^2	Spherical model, C_R of 1.8, SRP area of 2.02m^2
Integrator	8(9) Variable Step Runge-Kutta	4th Order Fixed Step Runge-Kutta
Integration Stepsize	1 second	10 seconds
Precession/Nutation Update Interval	1 second	10 seconds
Maneuver Model	Finite burns	Accelerometer measurements averaged over 10 seconds, including acceleration knowledge errors

PHASE 1 TEST

The Phase 1 test validates the receiver's performance during the 24hr period MMS-Phase 1 orbit, where the spacecraft make scientific observations in the Earth's dayside magnetopause. There are two maneuvers which Navigator must compensate for during this test. This is done by passing accelerometer data to the GEONS filter during the simulation. Since several orbits are required to fully validate the receiver performance, the Phase 1 test is run for a minimum of five days.

The simulated Phase 1 trajectory begins with the spacecraft approaching perigee at an altitude of about 4 R_E allowing the reception of many strong signals early in the simulation. GEONS is initialized with a valid point solution that has a geometric dilution of precision (GDOP) of 5.0 or less. This helps ensure that a reasonably good state is used to initialize the Kalman filter.

Figure 5 shows a quickly converging PPS error. The PPS error is a measurement Navigator's timing accuracy with respect to true simulation time. There is a residual uncompensated line-bias of about 125ns and a maximum variation of about 50ns, which primarily consists of quantization of the PPS pulse edge to one of the receiver's digital clock edges. The periodic nature of the errors coincides with the orbital period, although in Phase 1 timing errors never grow significantly because the filter is able to accurately model the USO and regularly has at least one measurement to process.

Figure 6 shows the real-time GEONS root sum-of-squares (RSS) position and velocity (PV) errors and filter one-sigma covariance estimates and Figure 7 shows the number of GPS signals tracked and orbital radius together. That the actual position and velocity errors are much smaller than the covariance estimates is expected and is the result of a conservative filter tuning. The periodic cycling of the error and covariance from maximum to minimum delineates the subsequent orbits as they progress from apogee to perigee and apogee again. The PV errors and filter covariance reach a minimum near perigee where the presence of many high quality measurements result in rapidly improved state estimates. The PV errors and filter covariance reach their maximum values before multiple GPS signals are tracked near perigee, and the maximum position error is less than 20 m RSS.

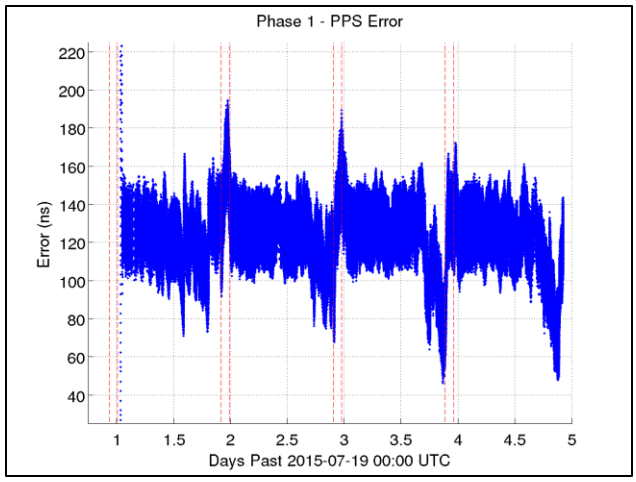

Figure 5: Phase 1 PPS error.

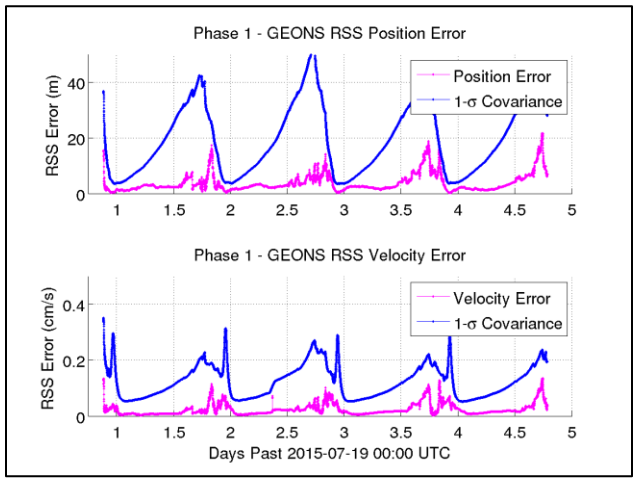

Figure 6: Phase 1 GEONS PV error and 1-σ covariance.

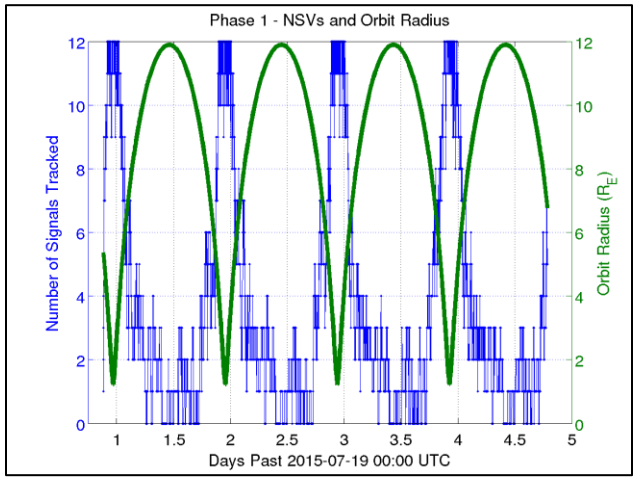

Figure 7: Phase 1 - number of signals used in GEONS solution, and orbit radius.

Figure 8 shows the error in the SMA estimate. The 100m requirement is easily met here, even in the region where the requirement is relaxed, below $3R_E$. Obvious spikes in SMA error occur as perigee is approached and the GEONS state is updated with new information from four GPS signals. Throughout the orbit, a strong correlation builds up between radius and speed error, and new information which is provided to the state estimator does not fit this correlation. This creates a transient in the estimate which is evident each time the spacecraft approaches a perigee after having tracked less than four GPS signal simultaneously for the majority of the previous orbital period. This topic is covered in detail by a recent article by *Carpenter, et al.* [**16**].

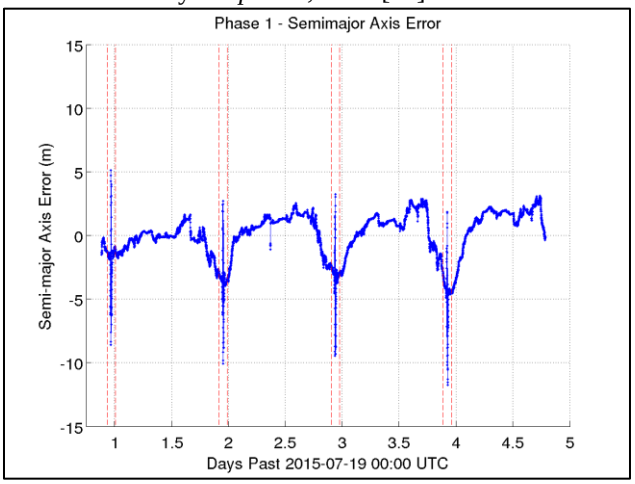

Figure 8: Phase 1 SMA error.

Figure 9 shows an example of the range of C/N_0 reported by Navigator as it exits perigee during the Phase 1 simulation. Notice the weak signals, identified with bold lines, which are successfully acquired and tracked in the presence of strong signals, the difference between some of which are greater than 15 dB (recall the dynamic range requirement). Acquiring and tracking weak signals in the presence of strong signals poses some difficulties which are discussed in the "Points of Interest" section found later in this paper.

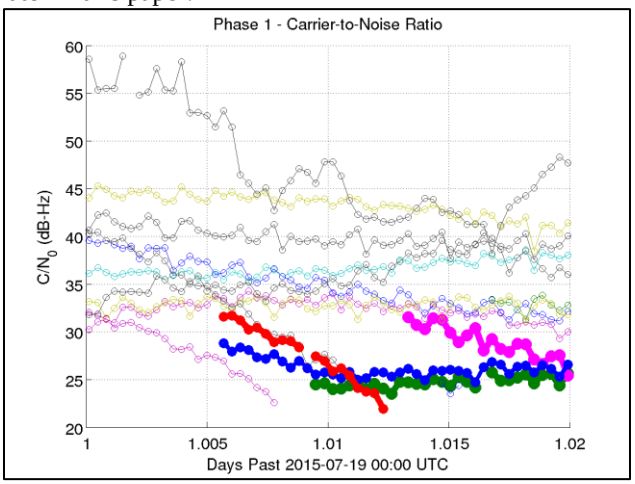

Figure 9: An example of the dynamic range of the C/N_0 reported by Navigator from the Phase 1 test.

PHASE 2 TEST

Once an apogee raising maneuver sequence is complete, the MMS constellation will be in its 2.8 day-long Phase 2 orbit where the spacecraft make scientific observations in the Earth's nightside magnetopause. The Phase 2 test is designed to verify performance in this regime. Again, since we require several orbits to validate the receiver performance, the Phase 2B test is run for a minimum of 8 days, but preferably for 14 days.

Again the simulation started with the spacecraft entering perigee at an altitude of $4R_E$. Figure 10 shows the PPS error over the duration of the Phase 2 orbit. As expected, the PPS error decreases rapidly as the simulated orbit moves through perigee and slowly grows as fewer signals are available at high altitude. Figure 11 shows the GEONS state estimate RSS PV errors and filter 1-sigma covariance. A small gap in the data around day 9 on the horizontal axis was due to a temporary failure of the GSE data collection equipment, but caused no major loss of information. As expected, the PV errors grow larger in the Phase 2 orbit than they do in Phase 1, reaching 50-100m and 0.25-0.75cm/s respectively. Still, all requirements are met with margin.

Figure 12 is analogous to Figure 7. Notice that, on average, at least one GPS signal is typically visible (although there are significant periods where no signals are tracked) even at apogee of $25R_E$ where the received signal power is below -171 dBW. Figure 13 shows the error in the estimated SMA is less than 18 m (as compared to the 100 m requirement in the RoI) after a two-perigee pass convergence period.

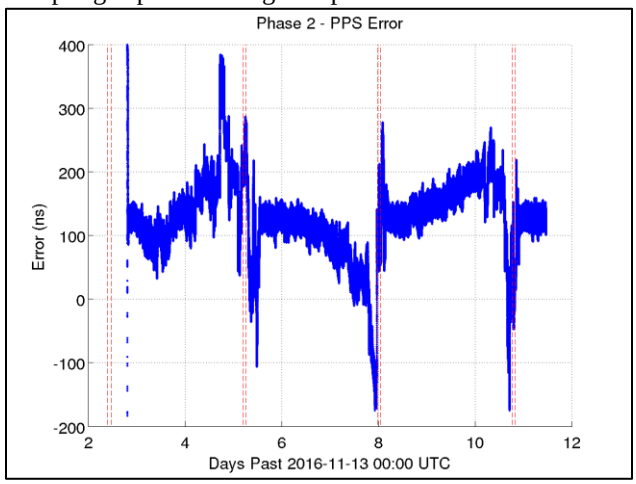

Figure 10: Phase 2 PPS error.

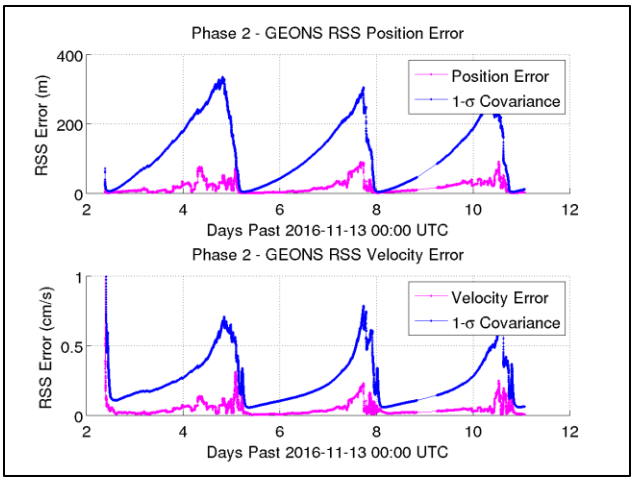

Figure 11: Phase 2 GEONS PV error and 1-σ covariance.

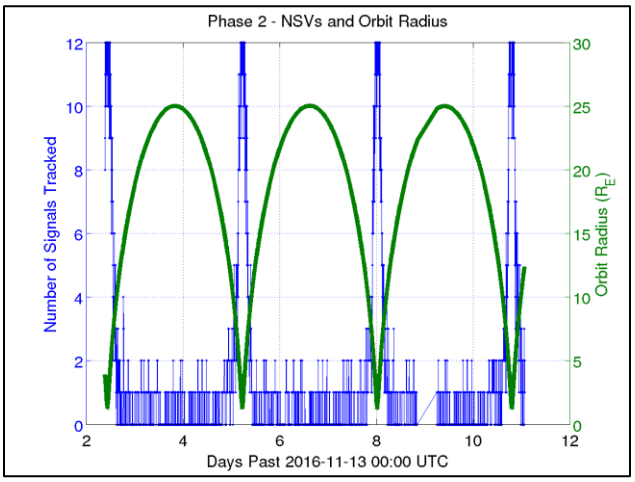

Figure 12: Phase 2 number of signals used in GEONS solution, and orbit radius.

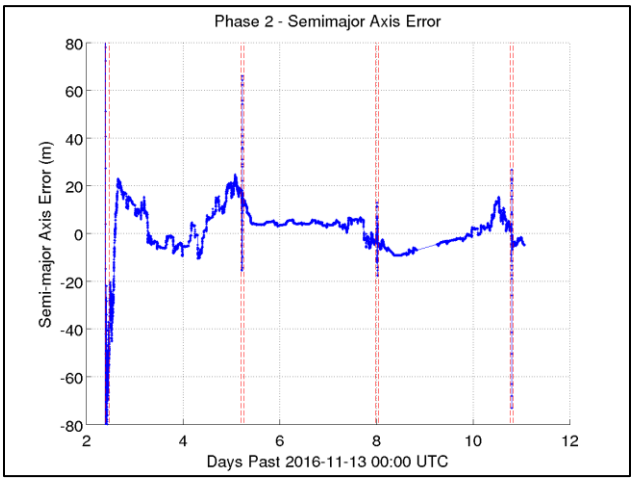

Figure 13: Phase 2 SMA error.

MEASUREMENT NOISE

The test plan also includes a measurement noise test that is designed to verify the pseudoranges produced by the receiver meet their noise requirements (<30m, 3-sigma).

To estimate the noise on the pseudorange measurements, a double-differencing technique is used to first remove signal dynamics by subtracting out the true dynamic and satellite clock (using information from the GPS simulator), and again differencing the single differenced measurements to remove receiver clock and other common errors [**17**]. Figure 14 demonstrates this process graphically.

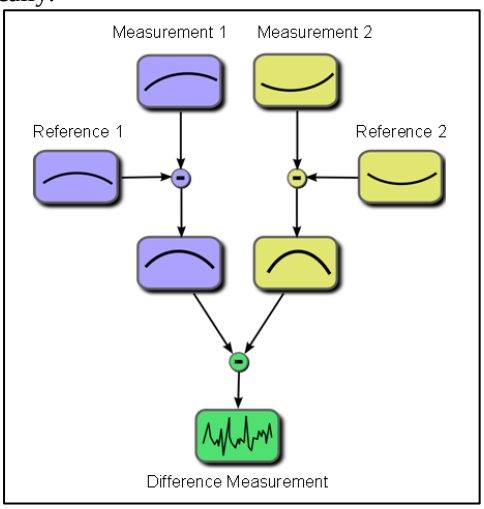

Figure 14: Measurement Noise test algorithm.

To ensure a sufficient number of samples throughout the range of expected power levels, a special simulator scenario was created. The Measurement Noise test scenario is broken into fourteen discrete 30-minute stages where the signal strength is progressively stepped down from -146dBW to -174dBW. Each stage employs an identical, repeated orbit segment with mission-typical dynamics.

Figure 15 shows the results of the test from MMS-Navigator Flight Receiver 1-Side A. The 3-sigma noise on the pseudorange measurements is at most approximately 24m near the lower limit of Navigator's tracking threshold of -174dBW. Also shown on the plot is the theoretical delay-lock-loop (DLL) tracking thermal noise using Equation 2 from [**18**].

$$\sigma_{tDLL} = \lambda_c \sqrt{\frac{4F_1 d^2 B_n}{c/n_0}\left[2(1-d) + \frac{4F_2 d}{T\, c/n_0}\right]} \qquad (1)$$

Here, λ_c is the wavelength of a GPS L1 C/A code chip (293.05 m/chip), F_1 is the dimensionless DLL discriminator correlator factor (½ for Navigator), d is the dimensionless correlator spacing between dedicated early, prompt, and late (EPL) correlators (½), B_n is the code loop noise bandwidth in Hertz (¼ Hz or ½ Hz), T is the predetection integration time in seconds (1 ms or 20 ms), and F_2 is the dimensionless discriminator type factor for EPL correlators (1). In Figure 15 one will notice a slight change in concavity of the DLL noise curve near -156 dBW, the weak signal threshold point. This is a result of the predetection integration time increasing from 1 ms to 20 ms and the DLL noise bandwidth B_n increasing from ¼ Hz to ½ Hz. That the receiver would choose to use a wider DLL bandwidth for weaker signals may seem counterintuitive, but it was observed to increase the probability of successfully initiating tracking of weak signals.

The measured pseudorange noise is reasonably close to, but generally exceeds the theoretical prediction by up to a factor of 2. While this discrepancy has not been studied in detail, a plausible explanation is that additional noise/stress is introduced in the antenna handoff process.

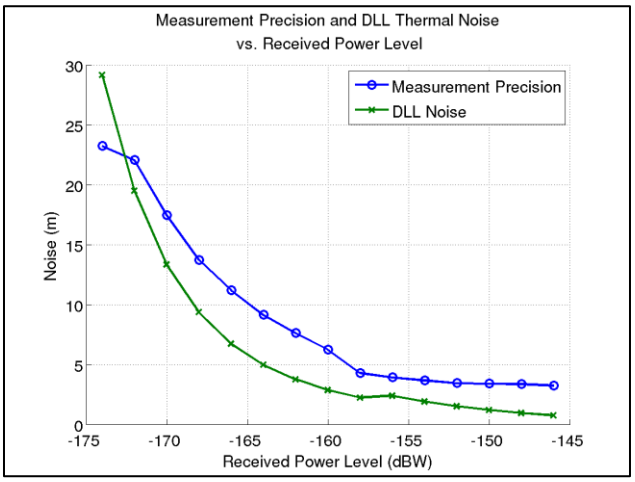

Figure 15: Three-sigma noise on the pseudorange measurements.

ACQUISITION PROBABILITY

In order to verify the MMS Navigator signal acquisition requirements, a special acquisition probability test was developed. At this point the reader should note that Navigator uses a dedicated Fast-Fourier-Transform-based acquisition engine to perform acquisition attempts rather than the common approach of configuring tracking channels in search mode. This test is designed to evaluate the performance of the acquisition engine and verify the receiver's ability to successfully handoff acquired signals to a tracking channel. The acquisition engine will normally only operate if there is a free channel to handoff acquired signals to, and in the presence of GPS signals empty channels are quickly filled. This limits the number of acquisitions attempts performed in normal operation. To ensure that a statistically significant sample of acquisitions could be collected in a reasonable amount of time, a special build of the Navigator software was developed to sidestep this issue. In this build, six of the receiver's twelve channels were configured to behave normally (i.e. acquire and track signals, compute point solutions, and send measurements to GEONS). The remaining six channels were configured specifically for the test to receive acquisition attempts. The acquisition engine was set up to attempt to acquire the signal being

tracked by channel number one (with Doppler predictions based on GEONS state estimates allowed for weak signals). The first channel's tracking state information (C/N_0, code phase, Doppler, information) was recorded and used as truth data. An acquisition was deemed successful only if a successful handoff from acquisition to tracking (to one of the second group of six channels) was achieved, and the tracking parameters matched the channel-one truth data. After a successful acquisition, the channel was cleared and the process restarted.

The MMS-Navigator uses two modes for acquisition: one mode is configured for speed, and the other for high-sensitivity. These are referred to as "strong" and "weak" acquisition modes, respectively.

The Acquisition Probability test software build is designed to make approximately equal numbers of strong and weak mode attempts. To get a wide range of signal levels with mission-typical dynamics, a Spirent simulation was configured to execute a segment of the Phase 1 orbit starting well above perigee, passing through, and then ending well above perigee again.

The resulting detection-probability vs. C/N_0 curves, separated by weak or strong mode, and the distribution of attempts are shown in Figure 16. Navigator's acquisition performance, which we take as the maximum of the red and blue curves dominates the black-dotted requirement line.

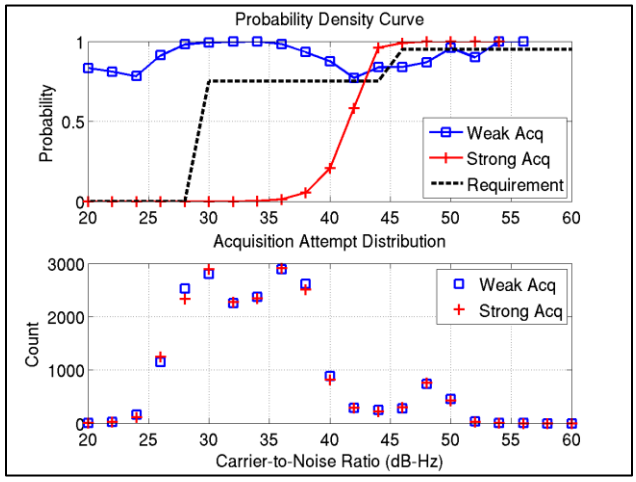

Figure 16: Acquisition characteristics.

MAXIMUM SPIN RATE

While the nominal spin rate of the MMS spacecraft is 3 RPM, unforeseen circumstances may prohibit the attitude control system from precisely controlling this rate. Furthermore, during the commissioning phase of the MMS mission, the spacecraft will spin at a much higher rate in order to aid in the deployment of booms and wires which will extend radially from the sides of the spacecraft.

In the course of regular performance testing, the spin rate was set to 3.4 RPM, with the signal moving from antenna to antenna approximately every 4.4 seconds. This slightly elevated spin rate provided a margin of conservatism in the full system test results, but the question remained as to how higher spin rates would degrade the receiver's performance. To answer this question we developed the maximum spin rate test.

Previous Spirent testing and theoretical considerations implied that the upper limit of Spirent's capacity for this type of antenna switching testing is between approximately 7.5 RPM and 10 RPM. Therefore, a Phase 1 Spirent scenario was created in which the spacecraft was spinning at 7.2RPM, allowing sufficient margin from the empirically derived limit of Spirent and also show Navigator can perform at much higher than nominal spinning rates. At 7.2 RPM, the handoff between antennas occurs approximately every 2.1 seconds.

As expected, Navigator's position and velocity errors are higher in these tests than during the nominal spin rate tests, because fewer GPS signals are tracked, as shown by Figure 17 and Figure 18. With fewer measurements available for GEONS, the covariance also remains higher. While the error in the SMA is apparently converged after the first perigee pass in the nominal spin-rate case (Figure 8), two passes are required for the filter to converge in the maximum spin rate test (Figure 19).

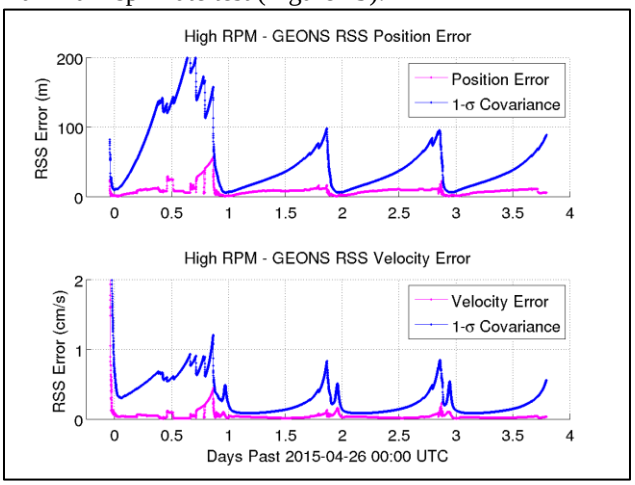

Figure 17: High RPM GEONS PV error and 1-σ covariance.

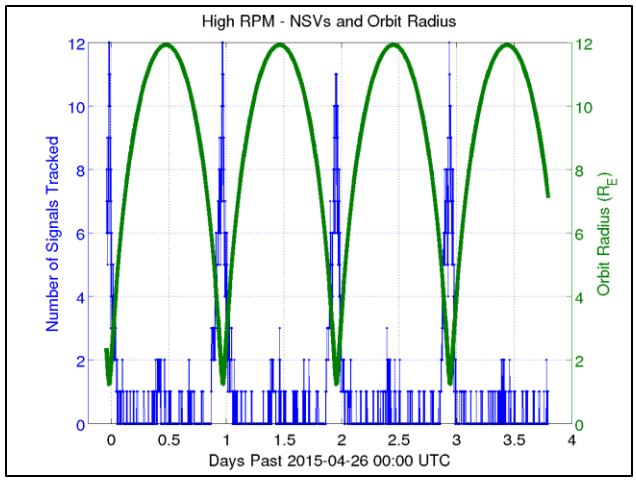

Figure 18: High RPM number of signals used in GEONS solution, and orbit radius.

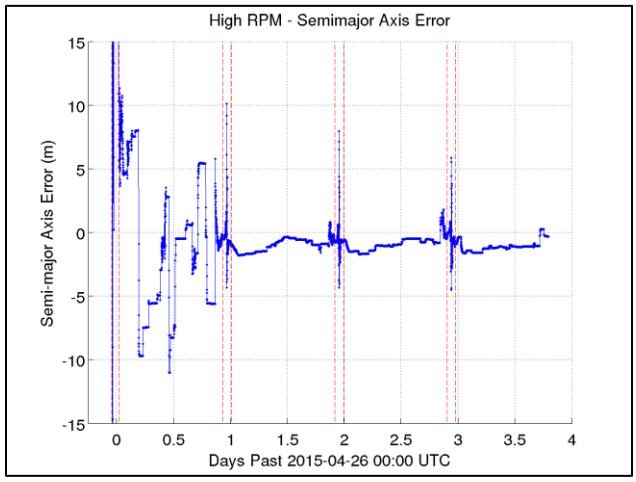

Figure 19: High RPM SMA error.

POINTS OF INTEREST

In addition to the baseline Navigator receiver capabilities such as weak signal tracking and survivability in high Earth orbits, the requirements of the MMS mission necessitated other advanced capabilities and customization. While the Navigator team has fully met the challenge, in early tests of the receiver erroneous measurements and large outliers were sometimes observed. Below, two primary causes for these outliers are discussed: cross-correlations (XC), and parity errors in decoding the GPS broadcast ephemeris. Also discussed are the implemented strategies to identify and prevent these problems from degrading receiver performance.

CROSS-CORRELATIONS

Cross-correlations occur when a GPS signal modulated with a particular pseudo-random noise (PRN) sequence is tracked with a different PRN sequence. Theoretically, the 1023-length GPS ranging codes provide at least 23dB of protection against XCs, but one may reasonably expect this protection to be reduced by 3 dB in the presence of noise [**19**]. Thus, given an acquisition sensitivity of 23-25dB-Hz or lower, signals with C/N_0 greater than about 46 dB-Hz pose a risk for being acquired and tracked as XCs. This risk is particularly high in the MMS-Navigator, which sees a high dynamic range of signal levels (23-55dB-Hz), and for robustness reasons, uses very little a-priori for acquisition, searching across large Doppler and delay swaths for strong and weak signals simultaneously.

Cross-correlation signals are troublesome as they prevent valid signals from using the channel and produce invalid measurements. While standard error checks in the point solution almost always edit these measurements (because their residuals are so large) the possibility remains that one could pass the error checks and cause performance issues.

Unfortunately the GPS broadcast message does not contain an explicit transmitter identification (SVID) field; otherwise this would provide an obvious way to detect XCs: check if the PRN sequence used for tracking corresponds to that assigned to the SVID providing data. Nonetheless the MMS-Navigator has developed a method of identifying cross-correlations from broadcast data. In this method the position of the tracked satellite (with its assumed SVID based on the PRN sequence being used for tracking) is computed at a common time using both the broadcast ephemeris downloaded from satellite and a trusted GPS almanac received from a strong signal. If the positions differ by more than 10km, the signal is declared a XC and removed from its tracking channel, otherwise it is "validated" as a good (non-XC) signal once and for all. A study of these position differences using three years of GPS archive data, showed this method to be very robust. In our method, we use the time of ephemeris (TOE) plus one half hour as the common time for position calculation. The half-hour offset ensures that the effects of certain ephemeris parameters are not "zeroed-out" in the comparison.

PARITY ERRORS IN NAVIGATION MESSAGE

At an orbital radius of $25R_E$ Navigator will track signals between 23-30 dB-Hz. These signals allow GEONS state estimates to converge faster and maintain a lower filter covariance. Signals tracked below 30dB-Hz make up 33% of the signals tracked during Phase 2. One of the problems with weak signals is the possibility of bit errors in decoding the navigation data message, and studies of MMS-Navigator telemetry have shown elevated bit error rates (for weak signals) due to cycle slips occurring in the antenna handoff process.

Bit errors are detected by the (32, 26) extended Hamming Code algorithm described in [**12**]. This algorithm only guarantees that four bit errors will be detected per 30 bits

decoded. Bursts of bit errors may cause the Hamming code to fail in a non-detectable way. Cycle slips may invert the bit stream somewhere in the middle of the 30 bits being parity checked, which can lead to a burst of bit errors that fail to be detected. Undetectable bit errors in parity checks may be seen either as unusual values in fields such as time of week, improper reserved bits, or incorrect ephemeris or almanac parameters, which can lead to large measurement errors.

To address the weak-signal bit error problem in the MMS-Navigator, the almanac data is not decoded from signals with a C/N_0 less than 30 dB-Hz, and ephemeris information is not used until it is verified that two decodes for a given issue of data ephemeris (IODE) are identical.

CONCLUSION

The MMS Mission Navigator GPS Receiver embodies over ten years of research and development in the area of high-altitude GPS navigation. The receiver has been designed specifically to meet and exceed the unique and challenging MMS requirements, which include the ability to acquire and track strong and weak signals (including those emerging from the side-lobes of the transmitter antenna patterns), maintaining continuous tracking of signals as they rise and set on each antenna of the spinning platform, and to operate robustly in the harsh, high-altitude space environment.

Developing the capability to test such a unique receiver represents a further challenge which has been met by Goddard's Formation Flying Testbed. The lab has been tailored to allow for efficient execution of the detailed test plan developed to verify the MMS-Navigator's requirements. This includes multiple, dual simulator configurations each with the capability to provide high fidelity RF stimulus for the MMS receivers. The simulator customizations include adapting Spirent simulators for spaceborne applications, implementing mission-specific receive antenna profiles, and fine-tuning global gain settings. Additionally, a suite of post-processing software has been developed to support performance verification. So far, three engineering test units and two of eight flight receivers have made their way through the lab.

Results have been presented for a subset of the flight tests executed on the first flight receiver. This includes two comprehensive full-system tests evaluating the performance in the two main MMS orbits, two benchmark tests, and a corner-case test. The performance of the receiver in these tests has been shown to meet all of its requirements with comfortable margin.

ACKNOWLEDGMENTS

The Navigator GPS receiver represents the dedicated work of many folks at GSFC. The authors recognize the efforts of the Navigator team in code 596, and thank J. Russell Carpenter and Michael Moreau for reviewing this paper.

REFERENCES

[1] W. Bamford et al., "GPS Navigator for the Magentospheric MultiScale Mission," in *Proc. of the ION GNSS*, Savannah, GA, 2009.

[2] L. Winternitz, W. Bamford, and G. Heckler, "A GPS Receiver for High-Altitude Navigation," *IEEE Journal of Selected Topics in Signal Processing*, vol. 3, no. 4, pp. 541-556, 2009.

[3] G. Heckler, L. Winternitz, and W. Bamford, "MMS-IRAS TRL-6 Testing," in *Proc. of ION GNSS*, Savannah, 2008.

[4] M. Moreau et al., "Results from the GPS Flight Experiment on the High Earth Orbit AMSAT AO-40 Spacecraft," in *Proc. of ION GPS*, Portland, OR, 2002.

[5] M. Dvorak-Wennersten et al., "PiVoT GPS Receiver," in *Proc. of ION GNSS*, Salt Lake City, UT, 2001, pp. 855-861.

[6] M. C. Moreau, "GPS Reciever Architecture for Autonomous Navigation in High Earth Orbits," University of Colorado, Boulder, Ph.D. Thesis 2001.

[7] W. Bamford and et. al., "A GPS Receiver for Lunar Missions," in *Proc. of ION NTM*, San Diego, 2008.

[8] C. Gramling, "Overview of the Magnetospheric MultiScale Formation Flying Mission," in *Astrodynamics Specialist Conference*, Pittsburgh, PA, 2009.

[9] K. Hsu, G. Skofronick-Jackson, C. D. Kummerow, and J. M. Shepherd, "Global Precipitation Measurement," *Precipitation: Advances in Measurement, Estimation and Prediction*, pp. 131-169.

[10] J. H. Klenzing, D. E. Rowland, J. Hill, and A. T. Weatherwax, "FIREFLY: A cubesat mission to study terrestrial gamma-ray flashes," in *Proc. of the AGU Fall Mtg*, 2009.

[11] T. Hitchens, Space Wars, March 2008.

[12] "Navstar GPS Space Segment/Navigation User Segment Interfaces," Global Positioning System Directorate, Specification IS-GPS-200F, 2011.

[13] Spirent SimGEN Software Users Manual, Issue 2-00.

[14] C. Olson, C. Wright, and Long A., "Expected Navigation Flight Performance for the Magnetospheric Multiscale (MMS) Mission," in *Proc. of 22nd AAS/AIAA*, Charleston, SC, 2012.

[15] P. Spindilaer, Magnetospheric MultiScale Mission Requirements Document.

[16] J. R. Carpenter and E. R. Schiesser, "Semimajor Axis Knowledge and GPS Orbit Determination," *Journal of ION*, vol. 48, no. 1, pp. 57-68, Spring 2001.

[17] G. N. Holt, G. E. Lightsey, and O. Montenbruck, "Benchmark Testing for Spaceborne Global Positioning System Receivers," in *Proc. of AIAA GNC*, Austin, TX, 2003.

[18] E. Kaplan, *Understanding GPS: Principles and Applications*.: Artech House, 1996.

[19] J. J. Spilker Jr., "GPS Signal Structure and Performance Characteristics," *Journal of ION*, vol. I, June 1989.